

Corrosion Protection from Inhibitors and Inhibitor Combinations Delivered by Synthetic Ion Exchange Compound Pigments in Organic Coatings

S. Chrisanti, K.A. Ralston, and R.G. Buchheit[†]

Fontana Corrosion Center, Department of Materials Science and Engineering,
The Ohio State University, Columbus, Ohio 43210 USA.

Inorganic ion exchange compounds (IECs) including hydrotalcites and bentonite clays are a well known classes of layered mixed metal hydroxides or silicates that demonstrate ion exchange properties. These compounds have a range of applications from water purification to catalyst supports. The use of synthetic versions of these compounds as environmentally friendly additives to paints for storage and release of inhibitors is a new and emerging application. In this paper, the general concept of storage and release of inhibiting ions from IEC-based particulate pigments added to organic coatings is presented. The unique aspects of the IEC structure and the ion exchange phenomenon that form the basis of the storage and release characteristic are illustrated in two examples comprising an anion exchanging hydrotalcite compound and a cation exchanging bentonite compound. Examples of the levels of corrosion protection imparted by use of these types of pigments in organic coatings applied to aluminum alloy substrates is shown. How corrosion inhibition translates to corrosion protection during accelerated exposure testing by organic coatings containing these compounds is also presented.

Keywords : coatings, ion exchange compounds, inhibitors, electrochemical impedance spectroscopy

1. Ion exchange compound as corrosion inhibiting pigments

Ion exchange compounds (IECs) including cation exchanging bentonites and montmorillonites, and anion-exchanging synthetic hydrotalcites (HTs) are important industrial materials used as absorbents, polymer stabilizers, catalyst supports, and neutralizing agents. For example, synthetic hydrotalcites are manufactured on an industrial scale with a manufacturing capacity that increased by at least 20,000 metric tons in 1999 alone.^{1,2)} Most of these applications exploit the unique nanostructure of HTs. Bentonites are commodity minerals used widely in a range of industrial applications, including use as an additive for paint.

Over the past five years we have developed a new application for IECs in the area of corrosion protection. We have shown that IECs can be synthesized into pigments that contain releasable anionic and cationic corrosion inhibitors. These pigments can be dispersed in organic resins and applied to metallic surfaces as a corrosion resistant

coating. In this paper, selected examples are given on the use of synthetic HT compounds to deliver anionic corrosion inhibitors, and synthetic bentonite and montmorillonites to deliver cationic inhibitors. The discussion will focus on an mixed Zn-Al hydroxide-decavanadate HT compound that releases Zn^{2+} and decavanadate as corrosion inhibiting species, and a Ce-bearing bentonite compound that releases Ce^{3+} as an inhibitor. The discussion will focus on corrosion protection of high strength Al alloys; specifically 2024-T3 (Al-4.4Cu-1.5Mg-0.6Mn).

1.1 Hydrotalcites

Hydrotalcite compounds consist of positively charged layers of mixed metal hydroxides separated by negatively charged layers of anions and water (Fig. 1). The prototypical HT compound is the naturally occurring hydro-magnesite whose formula is $Mg_6Al_2(OH)_{16} \cdot CO_3 \cdot 4H_2O$.^{3,4)} Structurally, the compound consists of $Mg(OH)_2$ layers. This layer is positively charged by substitution of trivalent Al on Mg sites. This positive charge is offset by negatively charged carbonate situated in the interlayer. Layer-to-layer spacing in HT depends in part on anion diameter,³⁾ and in some cases x-ray diffraction can be used

[†] Corresponding author: buchheit.8@osu.edu

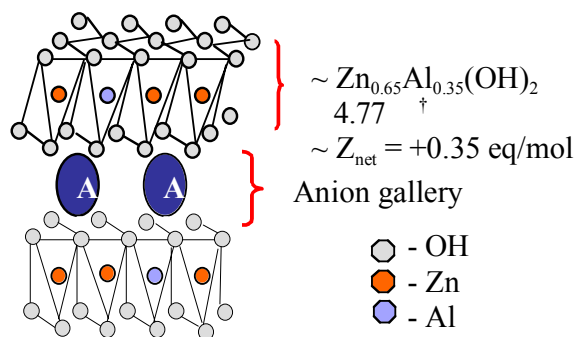


Fig. 1. Schematic illustration of the layered structure of anion-exchanging hydrotalcite clays.

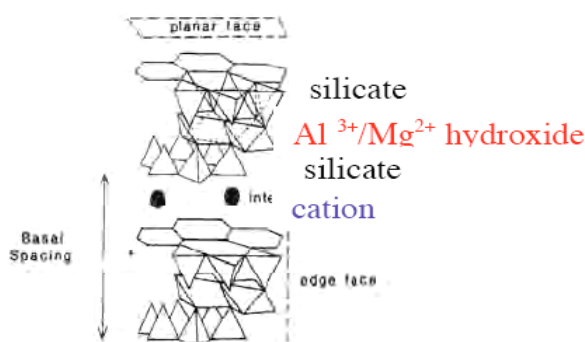


Fig. 2. Schematic illustration of the layered structure of cation-exchanging bentonite clays.

to provide information on the chemical identity of anions in the interlayer.³⁾

There is great chemical variety in HTs because there are many different pairs of metals that can combine to form the positively charged layered hydroxide "host". In turn, each host structure can accommodate many different types of anions. Hydrotalcite compounds may be synthesized as powders by titration one metal salt solution with another to induce co-precipitation.⁵⁾⁻⁷⁾

1.2 Bentonites

Bentonite is a hydrated alumino silicate clay primarily composed of the smectite mineral montmorillonite.⁸⁾ Fig. 2 is a schematic illustration of the smectite structure. Smectite is composed of units consisting of two silica tetrahedral sheets with a central alumina octahedral sheet.⁹⁾ The ideal chemical formula for montmorillonite is $(\text{Na}, \text{Ca})_{0.33}(\text{Al}_{1.67}, \text{Mg}_{0.33})\text{Si}_4\text{O}_{10}(\text{OH})_2 \cdot n\text{H}_2\text{O}$.⁸⁾ Isomorphic substitution of Al^{3+} with Mg^{2+} alters the crystal charge balance, giving the lattice a net negative charge. This requires adsorption of cations, commonly Na^+ and Ca^{2+} for charge balance.⁸⁾ The hydration of these exchangeable interlayer cations causes the bentonites to expand upon wetting. Therefore, layer separation in smectites depends

both on the interlayer cation and the amount of water associated with it.¹⁰⁾ The interlayer cations are much more accessible than other cations in the structure and can be exchanged with cations in solution when the clay is wetted by a salt solution.¹⁰⁾

1.3 Ion exchange

Ion exchange is the basis of the inhibitor release from IEC pigments in organic coatings. Anions in hydrotalcites may exchange with anions in a contacting solution while the host structure remains stable. Similarly, cations in bentonites can exchange with cations in solution without collapse of the host structure. Exchange reactions are regularly employed to embed large electrochemically or catalytically active anions in HT.¹¹⁾⁻¹³⁾ Their ability to participate in exchange reactions also makes these compounds useful anion scavengers.¹⁴⁾ Exchange isotherms and equilibrium constants have been measured for simple mono- and divalent anions such as Cl^- , F^- , SO_4^{2-} , and CO_3^{2-} , etc. exchanged with NO_3^- .¹⁵⁾ These equilibrium constants range from about -0.6 to 2.0 and tend to increase as the anion radius decreases and as anion valency increases. Exchange capacities are reported to range from 1 to 5 meq/gram making IECs very efficient inorganic ion scavengers.^{5),15)} Exchange characteristics also depend on the charge density in the host structure.¹⁶⁾

2. Synthesis approaches for ion exchange compounds

2.1 Hydrotalcites

Hydrotalcites can be synthesized by co-precipitation from aqueous solution. Generally, co-precipitation involves titrating a mixed metals salt solution with a solution containing the exchangeable anion while carefully controlling solution pH. A method described by Kooli is an example of how co-precipitation may be used to form a Zn-Al-hydroxide hosts intercalated with decavanadate, $\text{V}_{10}\text{O}_{28}^{6-}$.¹⁷⁾ First, 2000 ml of 0.33 M NaVO_3 solution is acidified from pH 8.5 to 4.5 by drop wise addition of 2 M HCl. At pH 4.5, the decavanadate anion ($\text{V}_{10}\text{O}_{28}^{6-}$) is speciated in solution, which is indicated by a change in the color of the solution from colorless to orange.¹⁸⁾ This anion is thermodynamically unstable at pH 6.5 (synthesis pH). However, the kinetics of transformation to the stable $\text{V}_3\text{O}_9^{3-}$ (metavanadate) anion are sufficiently slow so as to not interfere with the HT synthesis.¹⁸⁾ A 2 M NaOH solution is added drop wise from a burette with a plastic stopper so that the pH increases steadily. At pH 6.5, the precursor (1000 ml of 0.39 M ZnCl_2 and 0.2 M $\text{AlCl}_3 \cdot 6\text{H}_2\text{O}$ solution) is added drop-wise with

NaOH to keep the pH between 6.3 and 6.5. Under these conditions the resulting precipitate is the Zn-Al-decavanadate hydroxalcalite. The resulting mixture is aged for several hours at 55°C, filtered and rinsed. X-ray diffraction is typically used to verify synthesis.

2.2 Bentonites

Bentonite clays in dry powder form are inexpensive commodity materials. Bentonite may be mixed in a solution containing an exchangeable cation to induce exchange with Na^+ in the clay. The resulting compound contains the inhibitor ion of interest and this ion itself can be exchangeable leading to inhibitor release from the bentonite material. A Cerium (III) bentonite has been obtained by repeatedly soaking 50 g of Na-bentonite for several hours in 500 mL of a 0.5 M CeCl_3 solution. The resulting pigments were washed until no Cl^- was detected by a AgNO_3 test. Again, x-ray diffraction may be used to measure a change in the diffraction pattern associated with the exchange of Na^+ for Ce^{3+} .

3. Inhibitor release from IECs

As corrosion-inhibiting pigments, IECs must be able to store and later release soluble corrosion inhibitors into electrolyte that permeates a coating system. In the most general sense, the exchange characteristics of the pigment must favor inhibitor release, the kinetics of inhibitor release must be sufficient to achieve critical concentrations needed for inhibition, and the total inhibitor reservoir contained in the pigment must be large enough to confer long-lasting corrosion protection.

The exchange of interlayer ions in IECs is evident in x-ray diffraction data collected from hydroxalcalites and bentonites exposed to chloride solutions. Fig. 3 shows x-ray diffraction patterns for a Zn-Al-decavanadate hydroxalcalite in the as-fabricated condition, and after exposure to NaCl solutions of various types for exposure times of 22 days. As the exchange process occurs, large decavanadate ions are released and smaller chloride ions are absorbed. The exchange of large for small ions in the interlayer results in a change of interlayer spacing that can be observed as the appearance of a new peak in the diffraction pattern.

A similar effect is observed in Ce-exchanged bentonite pigments. Fig. 4 shows the x-ray diffraction pattern from a coating comprised of a 10 % by weight Ce-exchanged pigment dispersed in a polyvinyl butyral resin and applied to a 2024-T3 substrate. Coated samples were exposed in a 5 weight % salt fog chamber at 35°C for various lengths of time indicated in the Figure. The diffracted peaks are those associated with the exchangeable cation layer in the

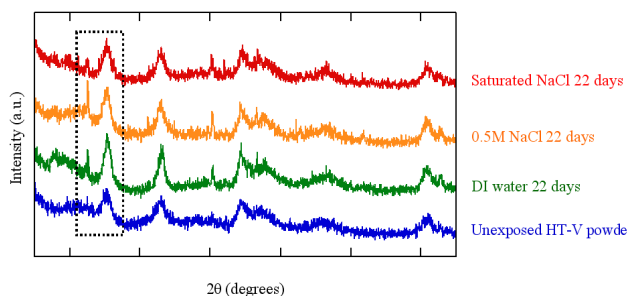


Fig. 3. X-ray diffraction pattern of Zn-Al-decavanadate hydroxalcalite pigments exposed to chloride solutions. The emergence of (003) peaks at $2\theta = 12^\circ$ is typical of chloride at the interlayer position in HT. The diffraction peak for the (006) planes associated with interlayer decavanadate occurs at $2\theta = 15^\circ$.

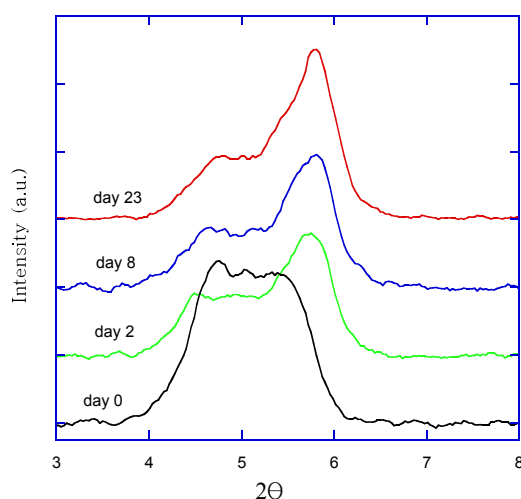
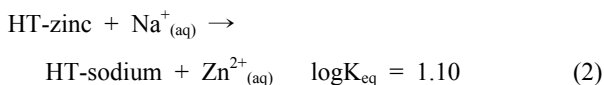
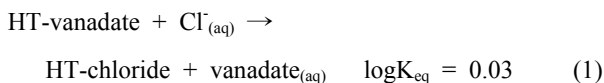


Fig. 4. X-ray diffraction patterns in the vicinity of the interlayer spacing diffraction peaks for bentonite. The peak at $2\theta = 5.8^\circ$ is associated with hydrated Na^+ ions. The peak at $2\theta = 4.8^\circ$ is associated with hydrated Ce^{3+} . As exposure time increases the intensity of the peak associated with Na increases compared to the peak associated with Ce^{3+} .

compound. Prior to exposure of the compound to a sodium chloride solution, the interlayer contains a mixture of Na^+ and Ce^{3+} ions because the exchange process used to impart Ce^{3+} does not result in complete exchange. As a result, the diffracted peak associated with Na^+ ($2\theta = 4.8^\circ$) is about the same intensity as that for Ce^{3+} ($2\theta = 4.8^\circ$). With increasing exposure time up to 23 days, the peak associated with a basal spacing determined by the incorporation of Na^+ ion increases relative to that of the peak associated with Ce^{3+} ion indicating Ce^{3+} release by Ce^{3+} -for- Na^+ exchange.

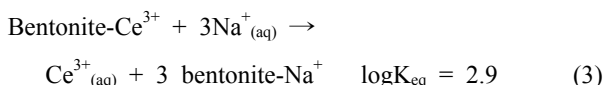
The extent of ion exchange between the solid and solution phase is characterized by an exchange isotherm. Exchange isotherms have been measured in pigment- sol-

ution equilibration experiments for the Zn-Al-decavanadate and Ce-exchanged bentonite.^{19),20)} When in contact with a dilute chloride solution. Zn-Al-decavanadate pigments release both Zn^{2+} and decavanadate according to the following reactions:



where HT-X (X = vanadate, chloride, zinc, and sodium) refers to the exchangeable species in the solid HT phase and the (aq) notation refers to ions in the solution phase. The small positive values for the equilibrium constants indicate that the forward reactions are slightly favored indicating a small thermodynamic driving force for release of the inhibitor.

In the case of Ce-exchanged bentonite, the exchange reaction in a chloride solution is given by:



The magnitude of the equilibrium constant for this exchange reaction is larger than those measured for exchange from Zn-Al-decavanadate hydrotalcite, and release of Ce^{3+} and uptake of Na^+ ions is favored.

In exposure experiments conducted over of several tens of hours, inhibitor release from both hydrotalcites and bentonites is mass transport limited.^{19),20)} Inhibitor release from pigments in coatings is also mass transport limited. Fig. 5 shows the concentration of vanadate and Zn^{2+} in solution released over hundreds of hours from a Zn-Al-decavanadate pigment loaded at a rate of 25% by weight into and epoxy resin and applied as a coating to Al alloy 2024-T3. The exposed area of the coating was 12.5 cm^2 and the volume of the solution was approximately 5 cm^3 and the vanadate and Zn^{2+} concentrations are plotted in the Fig. as a function of exposure time. Concentrations of the inhibitors were determined by inductively couple plasma-optical emission spectroscopy. This particular cell also contained 12.5 cm^2 of a bare 2024-T3 that may have been a sink that consumed soluble inhibitor released into solution. Fig. 5 shows that the concentration of Zn^{2+} developed in solution is several tens of parts per million by weight and compares with concentrations of Sr^{2+} cations released from a SrCrO_4 -pigmented

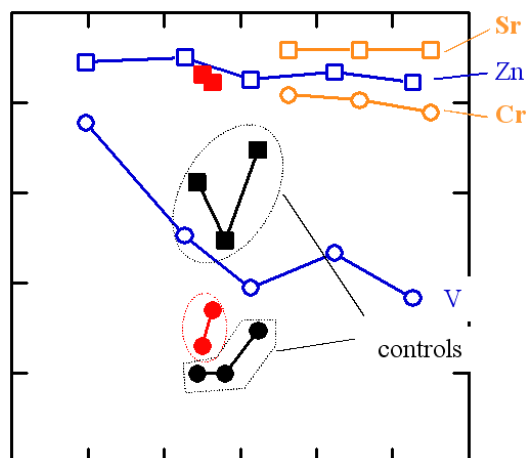


Fig. 5. Inhibitor concentrations developed as a function of exposure time in 5 cm^3 of 0.5 NaCl solution in contact with 12.5 cm^2 of an epoxy coating containing 25% by weight Zn-Al-decavanadate pigment applied to 2024-T3.

primer applied to 2024-T3 and evaluated in a comparable manner. Initially, the vanadate concentration developed in solution is measured to be nearly 10 ppm by weight, which approaches the concentrations of chromate released from a SrCrO_4 -pigmented primer. The vanadate concentration decreases with exposure time, perhaps due to adsorption or precipitation on the bare metal surface present in the exposure cell used in this particular experiment. The control data points shown in Fig. 5 show the concentrations of vanadate and Zn^{2+} developed by dissolution of 25 cm^2 of 2024-T3 in contact with 5 cm^3 of 0.5 M NaCl solution.

Fig. 6 characterizes inhibitor release from Zn-Al-decavanadate hydrotalcite and Ce-bearing bentonite using an x-ray diffraction approach. In this plot, the y-axis is the ratio of the intensity of diffracted peak associated with the spacing of the interlayer containing the exchangeable ion. The ratio plotted is that of the peak intensity at some exposure time normalized by the peak intensity at zero exposure time. As inhibitor is released from the interlayer, the volume fraction of the compound containing the inhibitor decreases and the intensity of the diffracted peak decreases. To facilitate plotting, the peak height ratio has been normalized to vary between 0 and 1. In the case of Zn-Al-decavanadate, the normalized peak height ratio varies little over the course of the experiment consistent with the small value of K_{eq} for the decavanadate-chloride exchange reaction shown in Eq. 1. In the case of Ce-exchanged bentonite, Ce appears to be released in two episodes. A period of rapid early release is followed by a regime characterized by slower diffusion-controlled exchange kinetics. The stimulated release demonstrated by

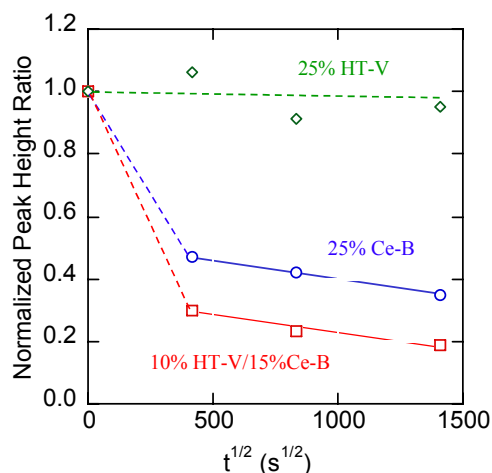


Fig. 6. Normalized peak height ratio versus exposure time. HT-V refers to a Zn-Al-decavanadate pigment; Ce-B refers to a Ce-exchanged bentonite. A data set for a mixed inhibitor combination is also shown. The PHR was computed from x-ray diffraction peaks associated with IEC interlayer spacing.

the Ce-exchanged bentonite also seems to be consistent with the larger K_{eq} value for the cerium-sodium exchange reaction of Eq. 3.

The total exchangeable capacity of inhibitor from an IEC pigment is important for determining the total useful life of the pigment and the coating containing it. The exchangeable fraction of an IEC can be assessed by serial washing experiments where an amount of pigment is washed with a fixed amount of solution. Assessments of inhibitor released into the washing solution, and the inhibitor remaining can be made. Total inhibitor release capacities for Zn-Al-decavanadate pigment exposed to dilute chloride solutions range from 1.2 to 2.2 mmol per gram for vanadate, and 0.13 to 5.9 mmol per gram for Zn^{2+} . The release capacity of Ce^{3+} from Ce-exchanged bentonite has not yet been estimated.

4. Examples of corrosion protection from coatings containing iec pigments

4.1 Salt spray exposure testing

Accelerated exposure testing is an important means of assessing the protectiveness of organic coatings. In an example of the levels of corrosion protection achievable with IEC pigments, Zn-Al-decavanadate and Ce-exchanged bentonite pigments were added to bisphenol epoxy resins to make rudimentary corrosion resistant coatings. These coatings were applied to degreased and deoxidized 2024-T3 substrates and cured. No conversion coating or adhesion promoter was applied to the surfaces prior to applica-

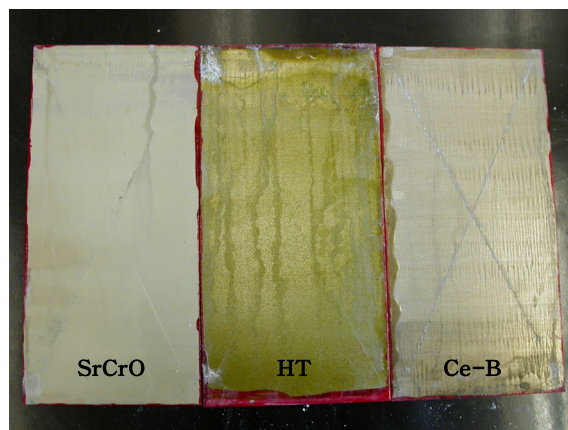


Fig. 7. Photograph of 2024-T3 samples coated using amide-cured epoxy resin doped with IEC pigments at a level of 25% weight after 1200 hours of ASTM B117 salt spray exposure. Samples were scribed prior to exposure. SrCrO₄: strontium chromate pigment; HT: Zn-Al-decavanadate pigment; Ce-B: Ce-exchanged bentonite pigment.

tion of the organic coating. Once cured, coated samples were scribed with a stylus to expose bare metal and subjected to exposure according to ASTM B117 (continuous spray generated from 5% NaCl solution, exposure temperature 35°C).²¹⁾ Periodically, samples were inspected visually for the presence of blisters and localized corrosion at defect sites in the coating. Samples were also inspected for corrosion damage in the scribe and corrosion under the coating initiated at the scribe. Results were compared to a SrCrO₄-pigmented epoxy primer applied per manufacturers instructions as a positive control.

Fig. 7 shows coated 2024-T3 samples after the 1200 hour exposure period. The SrCrO₄-epoxy coated sample shows no blistering or local corrosion through the coating. The bare metal in the scribe was bright suggesting powerful protection from chromate inhibitor released from the SrCrO₄ pigment. There is some minor staining from corrosion occurring at an unprotected edge of the sample. Overall, the corrosion protection provided by the SrCrO₄-epoxy coating is excellent as expected. The Zn-Al-decavanadate-epoxy coating also provides good protection to the underlying substrate, though not as good as that of the chromated coating. This sample presents no blistering or localized corrosion, The scribe is bright indicating protection by released inhibitors. There is a greater degree of corrosion at exposed sample edges that contributes to more staining and a degraded visual appearance compared to the positive control. The coating containing the Ce-exchanged bentonite also appears to provide a significant amount of corrosion protection. No blistering or localized corrosion is evident. Cut edge corrosion is minimal, but

white corrosion product is present in the scribe suggesting that any released Ce^{3+} is not effective in scribe protection under salt spray exposure conditions. These simple observations indicate that the corrosion protection provided by IEC-pigmented coatings is good. In the case of the Zn-Al-decavanadate-bearing coating, protection of bare metal in the scribe is evident. However, the overall impression is that the $SrCrO_4$ -pigmented coating corrosion protection is superior to that provided by either IEC-pigmented coating.

4.2 Characterization of protection by electrochemical impedance spectroscopy (EIS)

Further distinctions in the levels of corrosion protection provided by IEC-organic coatings can be drawn using EIS methods. Fig. 8 shows Bode magnitude and Bode phase angle plots of EIS data collected from each of the coatings presented in Fig. 7. Spectra were collected after 100 hours and 600 hours of salt spray exposure. To collect the spectra, samples were removed from the chamber, fitted with a clamp-on cell that permitted a section of the coating away from the scribe to be flooded with a 5% NaCl solution. The cell was fitted with counter and reference

electrode so that a conventional three-electrode controlled potential electrochemical impedance measurement might be made. Once a spectrum was collected, the samples were returned to the chamber for further testing.

The EIS data show notable differences in how the coatings provide protection. The spectra collected from the sample with the $SrCrO_4$ -pigmented coating show very little change from 100 to 600 hours of exposure. The spectra are characterized by a resistive response at high frequencies and a strongly capacitive response at low frequencies. Spectra collected within the first few hours of exposure show a well articulated coating capacitance and resistive plateau associated with a pore resistance. Because the $SrCrO_4$ coating, a commercial formulation, is loaded with additional extenders and additives, the coating permeability is very high allowing rapid water uptake. The causes a sharp decrease in the pore resistance, which effectively "shorts" the coating capacitance leading to a broad resistive plateau seen in Fig. 8. The presence of a broad capacitive region at lower frequencies indicates that the metal substrate is passive and not corroding to any great extent. It may be concluded that in this case the coating is saturated with solution, the metal coating interface is

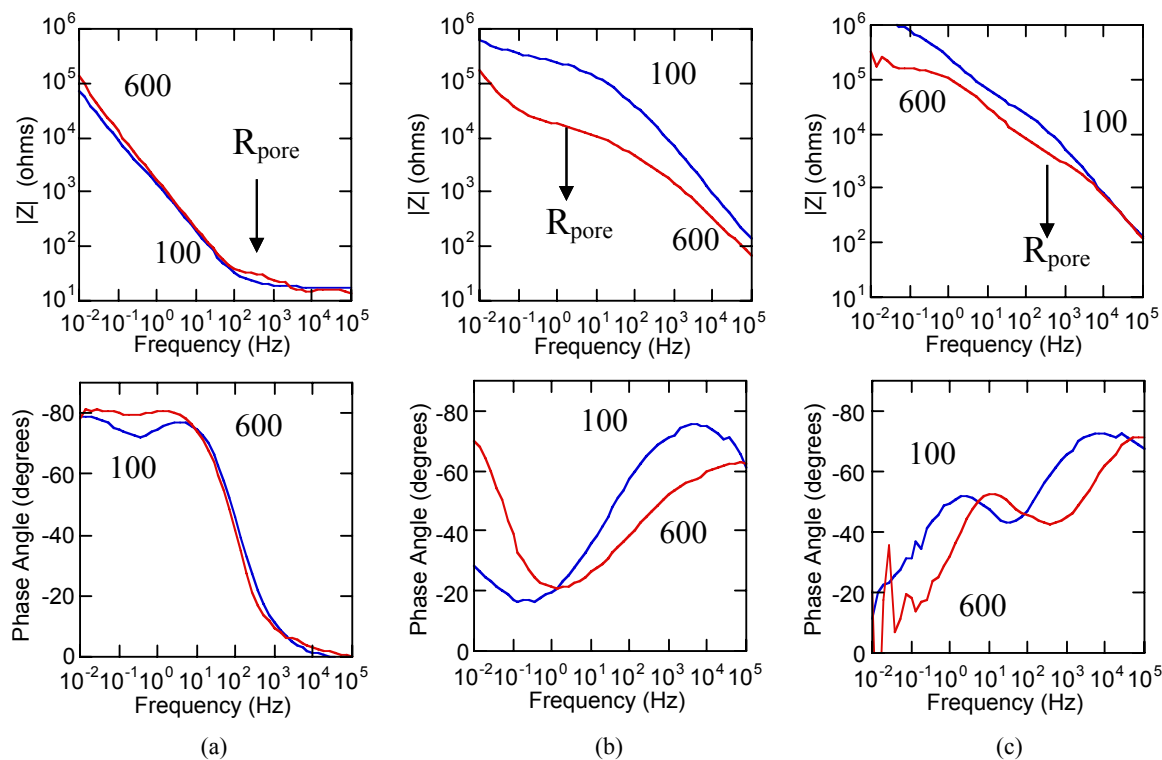


Fig. 8. Bode magnitude and phase angle plots for 2024-T3 with coatings pigmented with $SrCrO_4$ (a), Zn-Al-decavanadate (b), and the Ce-exchanged bentonite (c). The notations "100" and "600" appear near the data collected after 100 and 600 hours of salt spray exposure respectively. R_{pore} denotes the region in the magnitude plot where a resistive contribution from a pore resistance is evident.

wet, but the substrate is passivated, presumably by chromate leached from the sparingly soluble SrCrO₄ pigment addition.

A different scenario is presented by the sample with the Zn-Al-decavanadate-pigmented coating. While the total impedance at the lowest measured frequencies is high, the impedance magnitude at low frequencies decreases from 100 to 600 hours of exposure. At high frequencies a capacitive region is detected due to the coating capacitance. After 600 hours of exposure the Bode magnitude in this region is shifted to lower impedances, which is consistent with effects that might be expected from slow water uptake by the coating. In a related way, the pore resistance decreases from 100 to 600 hours. From the shifts in the coating capacitance and the pore resistance, it may be concluded that electrolyte is taken up more slowly by this coating compared to the SrCrO₄-pigmented coating. This is not surprising because the only solids addition to this experimental coating is the 25% IEC addition. It is interesting to note the increase in phase angle from 100 hours to 600 hours suggests a more capacitive response at the longer exposure time. Such a trend would be consistent with passivating action on the substrate by inhibitors released from the IEC pigment addition.

The EIS response of the sample coated using the Ce-exchanged bentonite formulation shares similarities with the coating pigmented with the hydrotalcite IEC. The total coating impedance decreases from 100 to 600 hours exposure. There is little change in the coating capacitance though a decrease in pore resistance is observed. Electrolyte uptake is occurring to some extent, but the effect on coating capacitance is not apparent. At the lowest frequencies the phase angle is low indicating that the impedance is dominated by a resistive component, which is an indicator of localized corrosion. Overall, these data suggest that this coating confers the lowest degree of corrosion protection of the three coatings compared.

5. Summary

Selected examples of the synthesis and use of ion exchange compounds illustrate their potential utility as corrosion inhibiting pigments for organic coatings. Simple aqueous processing methods can be used to create a range of synthetic IECs. These compounds allow specific inhibitors or inhibitor mixtures to be imparted to protective coatings. Inhibitors can be stored within IECs and released slowly and as needed as the environment penetrates the coating system. Exposure and electrochemical testing of organic coatings containing IEC pigments suggest that in-

hibiting properties are imparted by the pigment additions. The levels of protection are not equivalent to those achieved by chromate-bearing coatings, but IEC-bearing coatings are currently unoptimized from a coating formulation perspective and further gains may be expected as the exploration and use of IECs as pigments in coatings continues to mature.

Acknowledgements

The support of Concurrent Technologies Corporation, Largo FL, and the Air Force Office of Scientific Research under MURI contract no. F49602-01-1-0352 is gratefully acknowledged.

References

1. Anon., *Chemical and Engineering News*, **77**, 12 (1999).
2. Anon., *Chemical Week*, **161**, 27 (1999).
3. S. Miyata, *Clay and Clay Miner.*, **23**, 369 (1975).
4. H. F. W. Taylor, *Min. Mag.*, **39**, 377 (1973).
5. K. Itaya and H. C. Chang, *Inorg. Chem.*, **26**, 624 (1987).
6. K. R. Poppelmeier and S. J. Hwu, *Inorg. Chem.*, **26**, 3297 (1987).
7. W. T. Reichle, *J. Catal.*, **94**, 547 (1985).
8. S. K. Kawatra and S. J. Ripke, *Materials Engineering*, **14**, 647 (2001).
9. R. E. Grim, *Clay Mineralogy*, 2nd ed., p. 78, McGraw-Hill (1968).
10. D. Dermats and M. S. Dadachov, *Applied. Clay Science*, **23**, 245 (2003).
11. M. A. Drezdson, *Inorg. Chem.*, **27**, 4628 (1988).
12. E. T. Iyagba, A Study of the Crystal Structure of Hydrotalcites and Their Catalytic Properties, University of Pittsburgh (1986).
13. I. Sissoko, E. T. Iyagba, R. Sahai, and P. Biloen, *J. of Solid State Chem.*, **60**, 283 (1985).
14. J. K. G. Panitz and D. J. Sharp, The Use of Hydrotalcite as a Chloride-Ion Getter for a Barrier Aluminum Anodization Process, SAND95-2300, Sandia National Laboratories, Albuquerque (1995).
15. S. Miyata, *Clay and Clay Minerals*, **31**, 305 (1983).
16. S. Miyata, *Clay and Clay Minerals*, **28**, 50 (1980).
17. F. Kooli and W. Jones, *Inorg. Chem.*, **34**, 6237 (1995).
18. C. F. Baes and R. E. Mesmer, The Hydrolysis of Cations, p. 138, Robert E. Krieger Pub. Co., 1986.
19. S. Chrisanti and R. G. Buchheit, work in progress (2007).
20. S. P. V. Mahajanam, Application of hydrotalcites as corrosion inhibiting pigments in organic coatings, The Ohio State University (2005).
21. Standard Practice for Modified Salt Spray (Fog) Testing, in Annual Book of ASTM Standards, Section 3, Wear Erosion; Metal Corrosion, E. R. F. Allen, Editor. 1999, ASTM: West Conshohocken, PA. p. 367.